












Characterization of aerosol plumes from singing and playing wind instruments associated with the risk of airborne virus transmission

Lingzhe Wang¹  | Tong Lin¹  | Hevander Da Costa¹ | Shengwei Zhu¹  |
 Tehya Stockman²  | Abhishek Kumar³ | James Weaver⁴ | Mark Spede⁵  |
 Donald K. Milton⁶  | Jean Hertzberg³  | Darin W. Toohey⁷  | Marina E. Vance³  |
 Shelly L. Miller³  | Jelena Srebric¹ 

¹Department of Mechanical Engineering, University of Maryland, College Park, Maryland, USA

²Department of Civil, Environmental, and Architectural Engineering, University of Colorado Boulder, Boulder, Colorado, USA

³Department of Mechanical Engineering, University of Colorado Boulder, Boulder, Colorado, USA

⁴National Federation of State High School Associations, Indianapolis, Indiana, USA

⁵Department of Performing Arts, Clemson University, Clemson, South Carolina, USA

⁶Maryland Institute for Applied Environmental Health, School of Public Health, University of Maryland, College Park, Maryland, USA

⁷Department of Atmospheric and Oceanic Sciences, University of Colorado Boulder, Boulder, Colorado, USA

Correspondence

Jelena Srebric, Department of Mechanical Engineering, University of Maryland, College Park, MD, USA.
 Email: jsrebric@umd.edu

Funding information

College Band Directors National Association (CBDNA); National Federation of State High School Associations (NFHS); National Association of Music Merchants (NAMM); D'Addario Foundation; Alabama Music Educators Association; American Choral Directors Association (ACDA); American School Band Directors Association (ASBDA); Arts Ed NJ; Athletes and the Arts; Association for Body Mapping Education; Association of Anglican Musicians (AAM); Association of Concert Bands, Barbershop Harmony Society; California Youth Symphony Association; Canadian Band Association (CBA); Choral Canada, Church Music Publishers Association (CMPA); College Orchestra Directors Association (CODA); Country Music Association Foundation; Fargo-Moorhead Orchestral Association; Florida Music Education Association (FMEA); French Musical Instrument Organisation (La Chambre Syndicale de la Facture Instrumentale, CSFI); Gala Choruses; Halifax Concert Band Society;

Abstract

The exhalation of aerosols during musical performances or rehearsals posed a risk of airborne virus transmission in the COVID-19 pandemic. Previous research studied aerosol plumes by only focusing on one risk factor, either the source strength or convective transport capability. Furthermore, the source strength was characterized by the aerosol concentration and ignored the airflow rate needed for risk analysis in actual musical performances. This study characterizes aerosol plumes that account for both the source strength and convective transport capability by conducting experiments with 18 human subjects. The source strength was characterized by the source aerosol emission rate, defined as the source aerosol concentration multiplied by the source airflow rate (brass 383 particle/s, singing 408 particle/s, and woodwind 480 particle/s). The convective transport capability was characterized by the plume influence distance, defined as the sum of the horizontal jet length and horizontal instrument length (brass 0.6 m, singing 0.6 m and woodwind 0.8 m). Results indicate that woodwind instruments produced the highest risk with approximately 20% higher source aerosol emission rates and 30% higher plume influence distances compared with the average of the same risk indicators for singing and brass instruments. Interestingly, the clarinet performance produced moderate source aerosol concentrations at the instrument's bell, but had the highest source aerosol emission rates due to high source airflow rates. Flute performance generated plumes with the

This is an open access article under the terms of the [Creative Commons Attribution-NonCommercial-NoDerivs](https://creativecommons.org/licenses/by-nc-nd/4.0/) License, which permits use and distribution in any medium, provided the original work is properly cited, the use is non-commercial and no modifications or adaptations are made.

© 2022 The Authors. *Indoor Air* published by John Wiley & Sons Ltd.

Indiana Choral Directors Association; Indiana State School Music Association; Indianapolis Children's Choir; International Double Reed Society (IDRS); International Music Council; Kansas Bandmasters Association (KBA); Kappa Kappa Psi; Kentucky Music Educators Association (KMEA); Lakeville Area Community Band; League of American Orchestras; Lesbian & Gay Band Association; Maine Music Educators Association (MMEA); Manitoba Band Association; Mid Penn Band Organization; Music Association of California Community Colleges (MACCC); Music for All; Music Learning Band Program; Music Teachers National Association (MTNA); Music Publishers Association; National Association for Music Education (NAfME); National Association of Teachers of Singing (NATS); National Collegiate Choral Organization (NCCO); National Guild for Community Arts Education; National Music Council of the US; National Speech and Debate Association (NSDA); New Horizons International Music Association (NHIMA); New York State Band Directors Association; New York State School Music Association (NYSSMA); North Carolina Music Educators Association; Nova Scotia Band Association; Oahu Band Directors Association; Ohio Foundation for Music Education (OFME); Ohio Music Education Association (OMEA); Opera America; Orcas Island Community Band; Orchestras Canada/Orchestres Canada; Organization of American Kodály Educators (OAKE); Performing Arts Medicine Association (PAMA); Phi Mu Alpha Sinfonia; Quadrant Research; Saskatchewan Band Association; Sigma Alpha Iota Philanthropies; Sing A Mile High International Children's Choral Festival; Slate Valley Singers; Songwriters Guild of America (SGA); South Dakota Bandmasters Association; South Dakota Music Education Association; Surrey Music Educators Association; Sweet Adeline's International (SAI); Tau Beta Sigma; Tennessee Music Education Association (TMEA); Texas Bandmasters Association; Texas Music Educators Association (TMEA); The College Music Society and The CMS Fund; The Main Street Singers, Inc. (Main Street Children's Choir); The National Catholic Band Association; The Sinfonia Educational Foundation; The Voice Foundation; Virginia Music Educators Association; Voice and Speech Trainers Association (VASTA); Wisconsin School Music Association; Women Band Directors International (WBDI); World Association for Symphonic Bands and Ensembles (WASBE); Young Voices of Colorado; ACC Band Directors Association; Big 12 Band Directors Association; Big 10 Band Directors Association; PAC 12 Band Directors Association; SEC Band Directors Association; Clemson University Bands; Linn-Benton Community College Bands; UCLA Bands; Utah State University Bands

lowest source aerosol emission rates but the highest plume influence distances due to the highest source airflow rate. Notably, these comprehensive results show that the source airflow is a critical component of the risk of airborne disease transmission. The effectiveness of masking and bell covering in reducing aerosol transmission is due to the mitigation of both source aerosol concentrations and plume influence distances. This study also found a musician who generated approximately five times more source aerosol concentrations than those of the other musicians who played the same instrument. Despite voice and brass instruments producing measurably lower average risk, it is possible to have an individual musician produce aerosol plumes with high source strength, resulting in enhanced transmission risk; however, our sample size was too small to make generalizable conclusions regarding the broad musician population.

KEYWORDS

aerosol plume, airborne disease transmission, flow visualization, particle image velocimetry, singing, wind instruments

1 | INTRODUCTION

The Coronavirus Disease 2019 (COVID-19) pandemic has led to a profound impact on music communities, with the total shutdown of music production and public events after a number of the outbreaks related to choir performances were reported in the U.S.,¹ Netherlands² Germany,³ France,⁴ Japan⁵ and South Korea.⁶ For example, on March 10, 2020, in Skagit Valley, Washington, following a 2.5-h rehearsal with 61 participants including a symptomatic index patient, 32 confirmed and 20 probable secondary COVID-19 cases were identified, including three hospitalizations and two deaths.¹ Aerosol transmission, which has been recognized as a primary route for COVID-19 spread by the World Health Organization (WHO) and the U.S. Center for Disease Control (CDC), was considered to account for the choir rehearsal outbreak in Skagit Valley, Washington,¹ due to much more aerosol being produced during singing than talking.^{7,8} During singing, aerosols are released with exhaled gas plumes.⁹ With the surrounding air continuously engaged, gas plumes are dispersed until completely mixing with the ambient air. With this process, aerosols will be continuously transported elsewhere by indoor air currents. Direct exposure to the exhaled gas plume from a SARS-CoV-2 virus carrier at a close distance will cause a high infection risk due to its high viral concentration. This study names the exhaled gas plume to be an "aerosol plume" to emphasize that it contains viral bioaerosols.

To prevent airborne disease transmission in musical performances, it is critical to know the extent of the aerosol plume generated by musical performances. The extent is determined by its interactions with thermal plumes around the human body and indoor ventilation flow.¹⁰⁻¹² Studies have characterized the aerosol plumes from speech,^{13,14} and from musical performances by focusing on the source strength, such as the aerosol concentration^{7,8,15-19} and the air velocity,^{18,20,21} or the convective transport capability, such as the transport distance.^{18,21-23} However, features were not integrated to provide a comprehensive characterization of aerosol plumes which could help develop effective infection control strategies covering all of the factors contributing to the aerosol transmission. Furthermore, the source strength was mostly characterized

Practical Implications

- Characterization of aerosol plumes and associated risk of airborne virus transmission during musical performances require both the source aerosol emission rate and plume influence distance.
- Woodwind instruments produced aerosol plumes with approximately 20% higher source aerosol emission rates and 30% greater plume influence distances compared to the average values of the same risk indicators for singing and brass instruments.
- Well-fitted masks are strongly recommended for singing because they can bring source aerosol concentrations to the background level in front of a singer and reduce plume influence distances by 65%.
- Bell covers with filters are strongly recommended for brass and woodwind instruments performances because they can bring source aerosol concentrations to the background level in front of the instrument bells and reduce plume influence distances by up to 57%.
- An individual musician could produce aerosol plumes with five times higher source aerosol concentrations than those of the other musicians who played the same instrument, resulting in enhanced transmission risk.

by the source aerosol concentration, ignoring the aerosol plume's source airflow rate needed for risk analyses.

This study investigated aerosol plumes from musical performances by considering both the source strength and convective transport capability to form a comprehensive characterization. In addition, the source strength was characterized by the source aerosol emission rate, defined as the source aerosol concentration multiplied by the source airflow rate. The convective transport capability was characterized by the plume influence distance, defined as the sum of the horizontal jet length and horizontal instrument length. An illustration of definitions of these aerosol plume characteristics is available in [Figure 1](#).

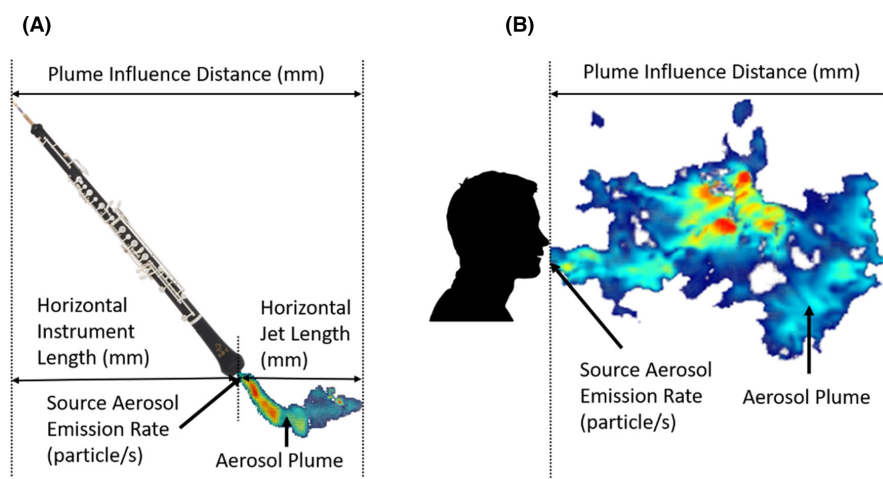


FIGURE 1 Description of terminologies in source strength and convective transport capability characterization of aerosol plumes from musical performances (A. Instrument, B. Singing)

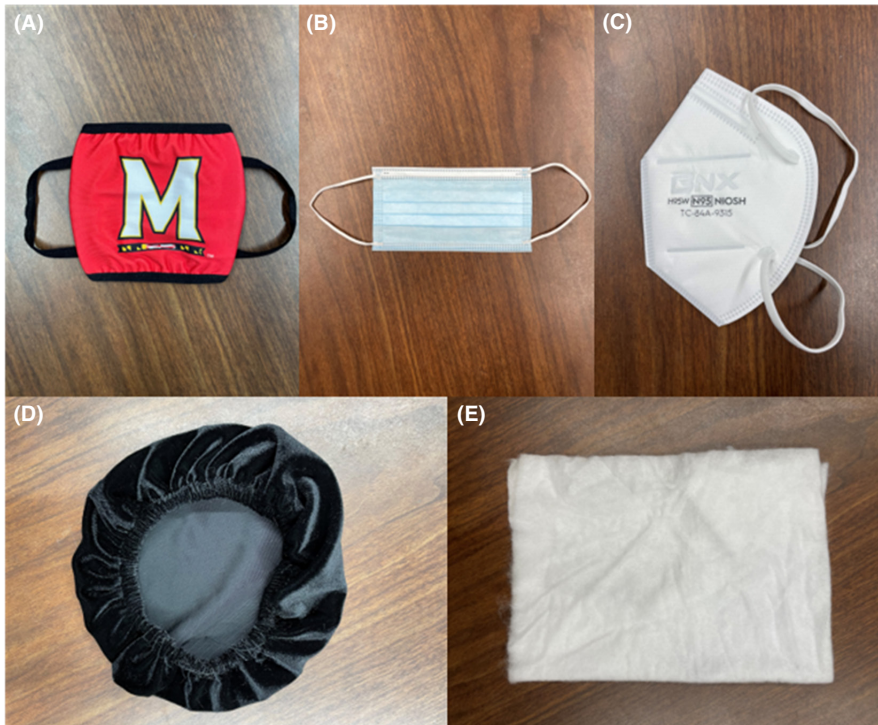


FIGURE 2 Mitigation Methods. (A) Cloth mask. (B) Surgical mask. (C) N95 mask. (D) Bell cover. (E) MERV-13 filter

TABLE 1 Human subject information

	Performance category	Participant numbers
Singing	Singing	4
Brass instrument	French Horn	3
	Trumpet	3
	Trombone	1
Woodwind instrument	Flute	3
	Clarinet	1
	Saxophone	2
	Oboe	1
Total		18

2 | METHODS

Human subject experiments with musicians were conducted under an approved Institutional Review Board protocol (IRB 1622465-4). In an environmental chamber, we conducted the source strength characterization by measuring the source aerosol concentration and the source velocity. At the same time, we conducted the convective transport capability characterization by visualizing the aerosol plume. This study also evaluated the performance of mitigation methods, including facial masks and bell covers. Cloth masks, surgical masks, and N95 masks were tested for singing. Bell covers alone and bell covers with MERV-13 filters were tested for playing instruments. The MERV-13 filters were used directly out of the packaging without any exposure to disinfecting agents such as alcohol. Masks, bell covers, and MERV-13 filters used in this study are shown in Figure 2. Experiments took place over roughly five months from November 2020 to March 2021. To protect researchers and

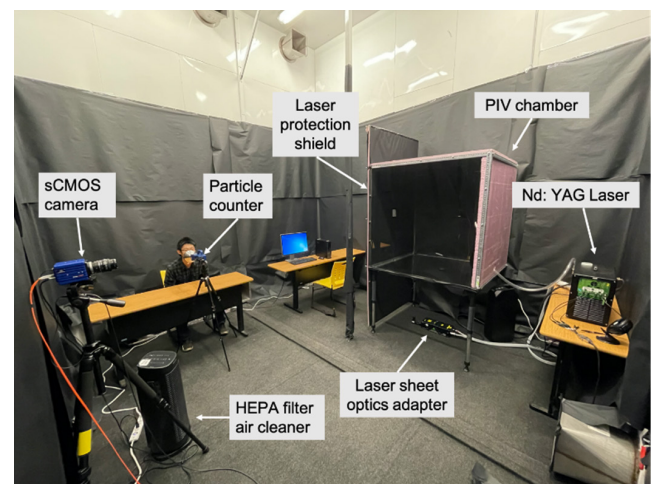


FIGURE 3 Environmental chamber setup

participants from COVID-19 infection, following procedures were implemented:

1. COVID-19 tests and COVID-19 screening surveys were completed by all researchers and participants within three days before the experiment, and only those with a negative test result could participate in the experiment.
2. Both researchers and participants were required to wear full personal protective equipment (surgical masks and gloves) and keep appropriate social distances (>6 ft) during experiments.
3. Before each experiment, the chamber was cleaned by wiping surfaces with alcohol-based disinfectants, mopping the floor with diluted bleach solutions, and running HEPA filter air cleaners to clean the room's air.

2.1 | Human subjects and experimental activities

The musicians in this study were upper-level undergraduate students or graduate students aged between 20 and 30, from the School of Music, University of Maryland. The experiment included 18 human subjects, representing most of the orchestra's aerosol-producing musicians, such as singing, French horn, trumpet, trombone, flute, clarinet, saxophone, and oboe. Detailed information of human subjects can be found in Table 1.

The music played by singers and instrument players was consistent for all experiments. Instrument players performed "Holt in E-flat for COVID-19 Study," which was specifically written for this study.¹⁸ It consisted of a slurred chromatic scale encompassing each instrument's normal range, and "Holt in Eb," which is a piece of music in the public domain. For singers, the music sample was "Holy, Holy, Holy," with the tempo to be 106 bpm. All musicians were instructed to keep their sound levels at approximately 70–90 dB. A sound level meter was visible to musicians to help control sound levels during experiments. Furthermore, at the experiment onset, each musician was asked to do a warm-up and practice the maintenance of the sound level. During the experiments, each musician was asked to repeat the same piece of music twice in a row without a rest interval. The duration of each musical performance was approximately one minute. Same procedures were conducted for mitigation method tests. Each musical performance was recorded as a time-series dataset, which was used to calculate the time-averaged values. The statistical analysis shown in the figures was conducted on these time-average values.

2.2 | Environmental chamber setup

Experiments were conducted in a climate-controlled chamber, which had a volume of 72 m³ (3.96 × 4.06 × 4.47 m). It was well sealed to minimize particle infiltration or exfiltration. The chamber mimicked a typical indoor environment for indoor rehearsal or performance spaces with air temperatures between 22 ± 2°C, relative humidity levels between 30% and 40%, and air velocities between 0.05 and 0.1 m/s. There was also a small cubic chamber for the particle image velocimetry (PIV) experiment, that is, PIV chamber, which had dimensions of 1.2 × 1.2 × 1.2 m. Figure 3 shows the setup of the environmental chamber.

2.3 | Experiments to characterize source strength

Two experiments were conducted to investigate the source strength of the aerosol plume from singing and playing wind instruments. One is to measure the source aerosol concentration and size distribution, the other is to measure the source velocity.

In our study, source aerosol concentration measurements deployed the particle counter (TSI 9306, Aerotrak) at the mouth of the singer or the bell of the instrument. The particle counter measures five particle size bins (0.3–0.5, 0.5–1, 1–3, 3–5, 5–10 μm). In each source aerosol



FIGURE 4 Source aerosol measurements with funnels for singing (left) and instrument (right)

concentration measurement, three air cleaners with HEPA filters were turned on one hour before measuring source aerosol concentrations to reduce the background particle concentration from approximately 800 to 0.5 particles/cm³. Air cleaners were kept on during measurements to ensure low background particle concentrations. In addition, air cleaners were placed at least two meters away from musicians to avoid interference with aerosol plume measurements. Each musician directed their aerosol plumes into a metal funnel to further minimize influences of the ambient air during source aerosol concentration measurements. The funnel was also used to help collect particles in the related experimental studies on exhaled aerosols.^{15,17,24–26} We prepared three funnels with diameters 10.4, 12.7, and 14.5 cm to fit various dimensions of the mouth and instrument outlet. The funnel was connected to the particle counter with a tube as short as 3 cm to minimize losses of particles due to adhesions to tube surface. To avoid interferences of ambient air entrainments, the funnel was placed as close as possible to aerosol sources, that is, the mouth or instrument outlet. The particle counter was fixed on a tripod when measuring exhaled aerosols from a singer, whose mouth was entirely covered by the funnel. When playing instruments, it was difficult to conduct measurements with the particle counter fixed on the tripod. Therefore, a researcher would hold it and ensure that the funnel could sufficiently capture expelled aerosols. If the bell of the instrument was smaller than the funnel, it would be entirely covered by the funnel. This was also the case for mouth measurements. If the bell was larger than the funnel, the funnel was placed inside the bell outlet without direct contact but with their centers aligned. Figure 4 illustrates aerosol measurements with funnels. Each measurement continued for the whole musical performance at one second sample interval for each trial.

The source velocity of aerosol plumes was measured by a hot-wire anemometer with an omni-directional probe (Kanomax 6543-2G, measuring range: 0.01–5 m/s). The velocity was measured at the center of a singer's mouth or an instrument's bell. To avoid the measurement error introduced by the movement of the participants during performances, a researcher held the probe to follow the movement of the singer's mouth or the instrument's outlet. The sampling interval was one second. Importantly, to avoid influence of the background environment, air cleaners were not running in this experiment.

The source airflow rate was calculated by multiplying the measured source velocity by the effective opening area available in

	Category	Effective opening area (cm ²)	Total area (cm ²)	Effective area percentage
Singing	Singing	3.40	3.40	100%
Brass instrument	French horn	6.90	515.39	1%
	Trumpet	5.27	71.13	7%
	Trombone	10.16	210.50	5%
Woodwind instrument	Flute End	2.84	2.84	100%
	Flute Mouth	1.00	1.00	100%
	Clarinet	9.38	29.64	32%
	Saxophone	9.19	99.36	9%
	Oboe	3.21	11.48	28%

TABLE 2 Effective flow area of musical performances

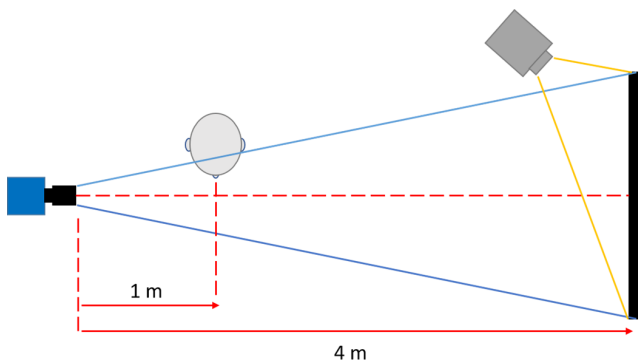


FIGURE 5 Description of BOS experiment setup

Table 2. The effective opening area calculation used the PIV flow visualization to identify mouth and bell areas discharging the airflow jet. This area is actually a cross-sectional area of the airflow jet at its source. Furthermore, we calculated the source aerosol emission rate by multiplying the source airflow rate with the source aerosol concentration. It was important to recognize that the singer/instrument airflow rates could be higher or lower than the sample airflow rate of the particle counter (0.047 L/s). If the source airflow rate was higher than the particle counter's sample airflow rate, some amount of the source airflow was bypassing the particle counter. In this case, the source aerosol concentration is equal to the aerosol concentration measured by the particle counter. If the source airflow rate was lower than the particle counter's sample airflow rate, the particle counter captured the entire source airflow, plus additional airflow from the ambient air that had a negligible particle concentration. The additional ambient airflow made the measured aerosol concentration to be lower than the source aerosol concentration. In this case, we derived the source aerosol concentration according to the mass balance of the particle counter's sampling volume.

2.4 | Experiments to characterize convective transport capability

This experiment visualized and derived the detailed information of aerosol plumes from the singing and instrument by utilizing

background-oriented schlieren (BOS) and particle image velocimetry (PIV).

The BOS system consists of four components: a scientific camera (sCMOS), a light, a BOS board made of four 2D BOS Random Dot Pattern Targets (1 × 1 m), and the BOS software. During measurements, the sCMOS camera was placed four meters away from the BOS board, and the participant was required to stand at one meter to the camera and three meters to the BOS board. Figure 5 shows the experiment setup of the BOS. The BOS visualized airflows by detecting density gradients between airflows and ambient air due to temperature differences. At each time step, the camera took two images with the second as the reference image to show the background (BOS board) without airflows. By comparing the two images, the certain pixel that appears at a different place was used to derive the density gradients.²⁷ In this study, it was not applicable to conduct BOS to visualize aerosol plumes from instrument performances because the temperature differences to the ambient air were too small to be used to detect density gradients. Thus, the BOS visualization was only conducted for the singers.

The PIV can provide detailed velocity distributions of aerosol plumes from singing and instrument performances. For a typical PIV recording, small tracer particles are added to the flow field. The plane of interest is illuminated twice by a laser light sheet. The light scattered by the tracer particles is recorded by a high-speed camera. The local displacement vector of the tracer particles of the first and second illumination is determined by the cross-correlation. Velocities are computed taking into account the time interval between two illuminations.²⁸

In this study, the measuring area was in the PIV chamber built with transparent plexiglass acrylic sheets (1.2 × 1.2 × 0.003 m) for the bottom and side walls, thick Styrofoam sheets (1.2 × 1.2 × 0.05 m) for the top and back walls, and thin Styrofoam (2.4 × 1.2 × 0.03 m) for the front wall. The front wall had an opening for exhaled aerosol plumes to flow through. The height and size of the opening were adjustable with respect to musical performances to fit the location and dimension of singers' mouths and instruments' bells. The front wall separated human subjects from the PIV measuring area to protect human subjects from laser hazards and avoid disturbances to aerosol plumes by ambient airflows, such as ascending thermal plumes and air movements caused by respirations. Front, top, back,

and side walls were covered by non-scattering black papers to avoid reflections of laser beams. The bottom was uncovered to let laser beams through. The wall faced to the camera was also uncovered, so that the camera could take photos for particles' movement highlighted by laser sheets. In addition, an airflow outlet was opened on the back wall, which helped maintain a constant pressure in the PIV chamber during measurements. The PIV system in our experiment was a 2D PIV, which captured the plane of the flow of interest. The test section was illuminated by a high speed pulsed Nd:YAG laser ($\lambda = 532$ nm) with a pulse intensity of 200 mJ. The light sheet thickness was 2.5 mm. To allow the laser emitting from bottom to top, the laser emitter was placed on the floor, under the bottom of the PIV chamber. Before the experiment, tracer particles (DEHS, mineral oil, 1 μm diameter) were generated by an aerosol generator and uniformly spread in the PIV chamber to achieve an optimal concentration. The PIV chamber made it possible to keep seedings at a relatively steady state during measurements. As the experiment started, the light scattered by tracer particles were captured by a high-speed camera (5.5 Megapixel scientific CMOS camera with double-frame mode for cross-correlation PIV) with an exposure of 15 μs . The camera faced perpendicular to the light sheet. The imaging frequency was 15 Hz, and the time interval between image pairs was set according to estimated velocities of exhaled airflow. The laser was aligned to the vertical midline of the opening on the front wall. The camera synchronized with the laser would record image frames of particles in the highlighted area of 0.76×0.64 m in size, and then, the processor would calculate velocity vectors with the 32×32 pixels interrogation window. The window had a 75% overlap and noise filtration with 5×5 Gaussian smoothing based on particles' moved

distances during the pulse interval.²⁸ During the experiment, participants were required to wear laser goggles for eye protection and to stand in front of the PIV chamber's front wall. They were requested to put their mouths against the opening of the front wall, or insert instruments' outlets into the PIV chamber. Figure 6 illustrates the PIV experiment setup. Specifications of measurement equipment can be found in Table 3.

2.5 | Data analysis

For the source strength characterization, the temporal data of source aerosol concentrations and source velocities collected at singers' mouths or instrument outlets were averaged over the period of musical performance to get the time-averaged data for each trial. The statistics were conducted on the time-averaged data of trials of musical performances. For the convective transport capability characterization, the maximum value of the jet length was selected from the temporal data over the period of musical performance for data analysis. Because of the limited sample size, outliers were defined to be further than $3 \times \text{IQR}$ (where IQR is the inter-quartile range, or the distance between the first and third quartiles). Most of the data were not normally distributed, so the Kruskal-Wallis H Test, which is a rank-based nonparametric test, was conducted to analyze the significance of difference between each group. The significant level α was selected to be 0.05. Python was used as the programming language for the data analysis. In figures, box and whiskers plots are for the statistics of measured data, bar charts are for calculated data.

3 | RESULTS

3.1 | Source strength characterization

Here, we present the source strength characterization of aerosol plumes from musical performances with source aerosol concentrations, source velocities, source airflow rates, and source aerosol emission rates as shown in Figures 7 and 8. For aerosol plumes generated by flute players, the source velocities at flautist's mouth and the end opening of the flute have noticeable differences. Thus, the measurements were conducted at both locations separately, as shown in Figure 7A. One French horn player generated much higher source aerosol concentration than the other players. This subject's data was categorized as "high shedder FH," "FH" represents the French horn. Given that a high source aerosol concentration influences the source aerosol emission rate, the data of the "high shedder FH" were shown both in Figure 7C,D.

Figure 7A compares source velocities of the aerosol plumes from musical performances and shows significant differences ($p = .013 < \alpha$). Note that the source velocity of the aerosol plume from the flautist's mouth was one to two magnitudes higher than those from the other instruments. Figure 8 shows the same data averaged over instrument categories. By treating the flautist mouth data as an

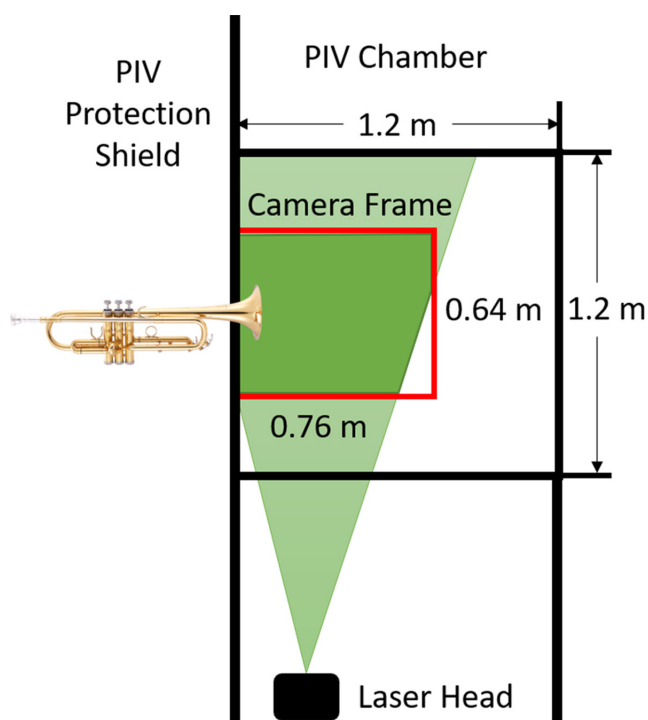


FIGURE 6 Description of PIV experiment setup

TABLE 3 Specifications of experiment equipment

Experiment	Equipment	Specification
Aerosol concentration measurement	Optical Particle Counter (TSI AEROTRAK 9306)	Channel Size: 0.3, 0.5, 1.0, 3.0, 5.0, 10.0 μm Counting Efficiency: 50% at 0.3 μm ; 100% for particles $>0.45 \mu\text{m}$
Air velocity measurement	Hot-wire Anemometer (Kanomax, ClimateMaster Series 6501 with 6543-2G probe)	Range: 0.01–5 m/s Accuracy: 0.01–0.99: ± 0.02 , 0.99–5.00: $\pm 2\%$
Background-Oriented Schlieren (BOS)	Background	Board with randomly distributed black squared dots on a white surface. Supplied by Lavision Inc.
	High-speed Camera	5.5 Megapixel scientific CMOS camera with Nikon 50 mm, F1.4. Supplied by Lavision Inc.
Particle image velocimetry (PIV)	Laser	Nd:YAG Dual Cavity pulsed laser, $2 \times 200 \text{ mJ}$ /pulse at 532 nm, 15 Hz imaging frequency. Supplied by Lavision Inc.
	High-speed Camera	5.5 Megapixel scientific CMOS camera with Nikon 50 mm, F1.4. Supplied by Lavision Inc.
	Processor	CPU: Intel(R) Xeon(R) W-2135 CPU @ 3.70 GHz, 6 cores Ram: 64 GB. Supplied by Lavision Inc.
	Aerosol Generator	DEHS (mineral oil, 0.91 g/cm^3 , 1 μm). Supplied by Lavision Inc.

outlier and excluding it from the dataset, Figure 8A shows the source velocity of singing was the highest. It was around three times higher than that of woodwind instruments and six times higher than that of brass instruments ($p = 1e-4 < \alpha$). Figures 7B and 8B show the source airflow rates of aerosol plumes. Overall, woodwind instruments—except for the oboe which uses a double-reed—generated higher source airflow rates than brass instruments. Figure 7C compares source aerosol concentrations of aerosol plumes from musical performances and shows significant differences ($p = 1.2e-5 < \alpha$) between categories. The source aerosol concentrations greatly varied in the orders of magnitude: 10^4 – 10^5 particles/L for the “high shedder FH” and trombone; 10^3 – 10^4 particles/L for trumpet, clarinet, oboe, French horn, singing, and saxophone; and 10^1 – 10^2 particles/L for flute. The size distribution of the source aerosol concentrations can be found in Figure 9. Figure 8C shows that the source aerosol concentration from brass instruments was about two times higher than that from singing and woodwind instruments ($p = .02 < \alpha$). Figure 7D shows the source aerosol emission rates of aerosol plumes. The clarinet had the highest source aerosol emission rate up to 1658 particles/s because of its relatively high source aerosol concentration and source airflow rate. Notably, due to the low source airflow rate of the French horn, the “high shedder FH” was ranked as first for the source aerosol concentration but second for the source aerosol emission rate. Figure 8D demonstrates that even though aerosol plumes of woodwind instruments had low source aerosol concentration, it still had about 20% higher source aerosol emission rates than the average of singing and brass instruments due to higher source airflow rates. These results illustrate that only measuring particle concentrations but ignoring source airflow rates will cause the

source strength characterization to be incomplete. Table 4 presents the measured data for the source strength characterization that also represent important boundary conditions for future numerical studies of musical performances.

3.2 | Convective transport capability characterization

For the convective transport capability characterization, aerosol plumes were visualized by particle image velocimetry (PIV) and background-oriented schlieren (BOS). During musical performances, we observed that the air jet was formed from the singer’s mouth or the instrument’s bell. It then left the outlet and traveled forward until it fully mixed with the ambient air. The plume influence distance was used for the convective transport capability characterization. It was defined as the sum of the instrument length and the aerosol plume’s jet length in the horizontal direction, which provided a reference distance from the end of the aerosol plume to the music player. This length can be used to assess the minimum social distance that should be used between players to keep them out of each other’s plumes. The horizontal jet length was defined as the farthest horizontal distance of the aerosol plume maintaining a velocity greater than 0.05 m/s. This demonstrates the extent of the area potentially having a non-negligible infection risk. For singing and instruments with bells close to the player’s body, such as the French horn and saxophone, the horizontal instrument lengths were treated as zero. The detailed instrument dimensions can be found in Table 5. Only the horizontal dimension was considered, as it is the main flow direction which

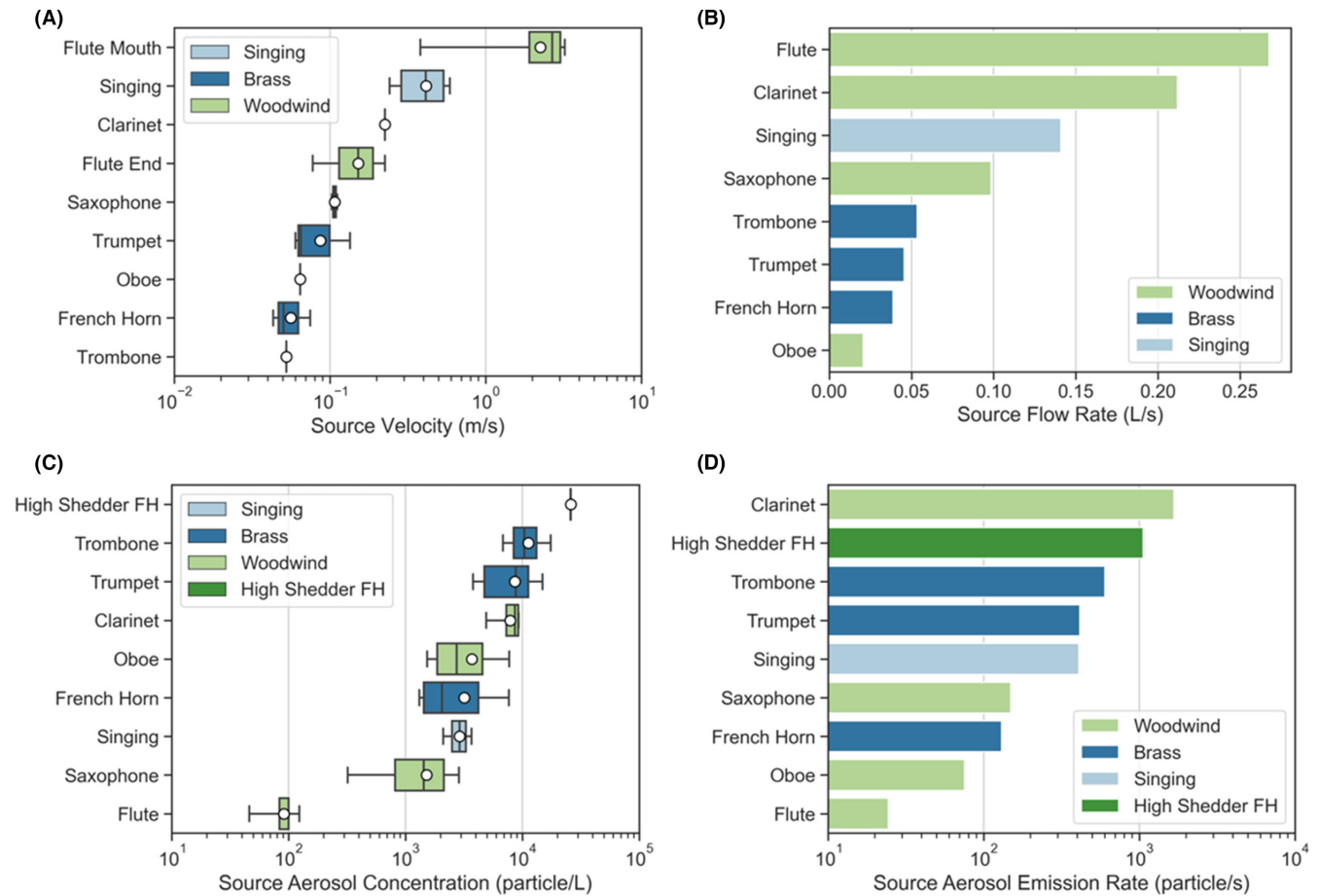


FIGURE 7 Source strength characterization of aerosol plumes from musical performances. (A) Source velocity. (B) Source airflow rate. (C) Source aerosol concentration including high shedder. (D) Source aerosol emission rate including high shedder. (note: “source” refers to the time-averaged data collected at singer mouth or instrument outlet)

influences the risk of the infection. The description of the features of convective transport capability characterization can be found in Figure 1.

During a performance, the horizontal jet length changed over time. The jets produced by playing a whole song were more dynamic than those by playing a single note. Figure 10 shows the fully developed jets moments before they were dissipated in the surrounding environment. We can see that the jets were complex and unsteady. The length and direction of the air jets by musical performances varied due to different instrument orientations and source velocities. To simplify the analysis of the complex time-dependent flow, the maximum jet lengths from performances were selected for the data analysis. From Figure 11A, jets of aerosol plumes produced from singing and playing the flute (both from the flautist’s mouth and flute end) horizontally traveled around 500 mm, farther than those from other instruments, which varied from around 100–400 mm. The differences were significant ($p = 1e-5 < \alpha$) between instruments. Figure 11B shows that the aerosol plume from singing had the longest horizontal jet length with an average of around 600 mm. The aerosol plume from brass instruments had the shortest horizontal jet length with an average

of 300 mm. The difference between each performance category was also significant ($p = 8.16e-7 < \alpha$). From Figure 11C, due to the longer jet length and long horizontal instrument length, the plume influence distance of playing flute reached about 1200 mm, which was clearly the farthest. Thus, the plume influence distance of woodwinds was about 30% greater than that of singing and brass instruments (Figure 11D). The data of plume influence distances can be found in Table 5.

3.3 | Comprehensive characterization

According to our findings, it is insufficient to independently study the source strength and convective transport capability because such an evaluation would provide incomplete understanding of risk from playing an instrument and singing. Here, we comprehensively characterized the aerosol plumes from musical performances by combining the source strength and convective transport capability to the comprehensive characterization factor. The weight of these two plume characteristics was set to be equal. The characterization factors were calculated based on the weighted sum method. Firstly,

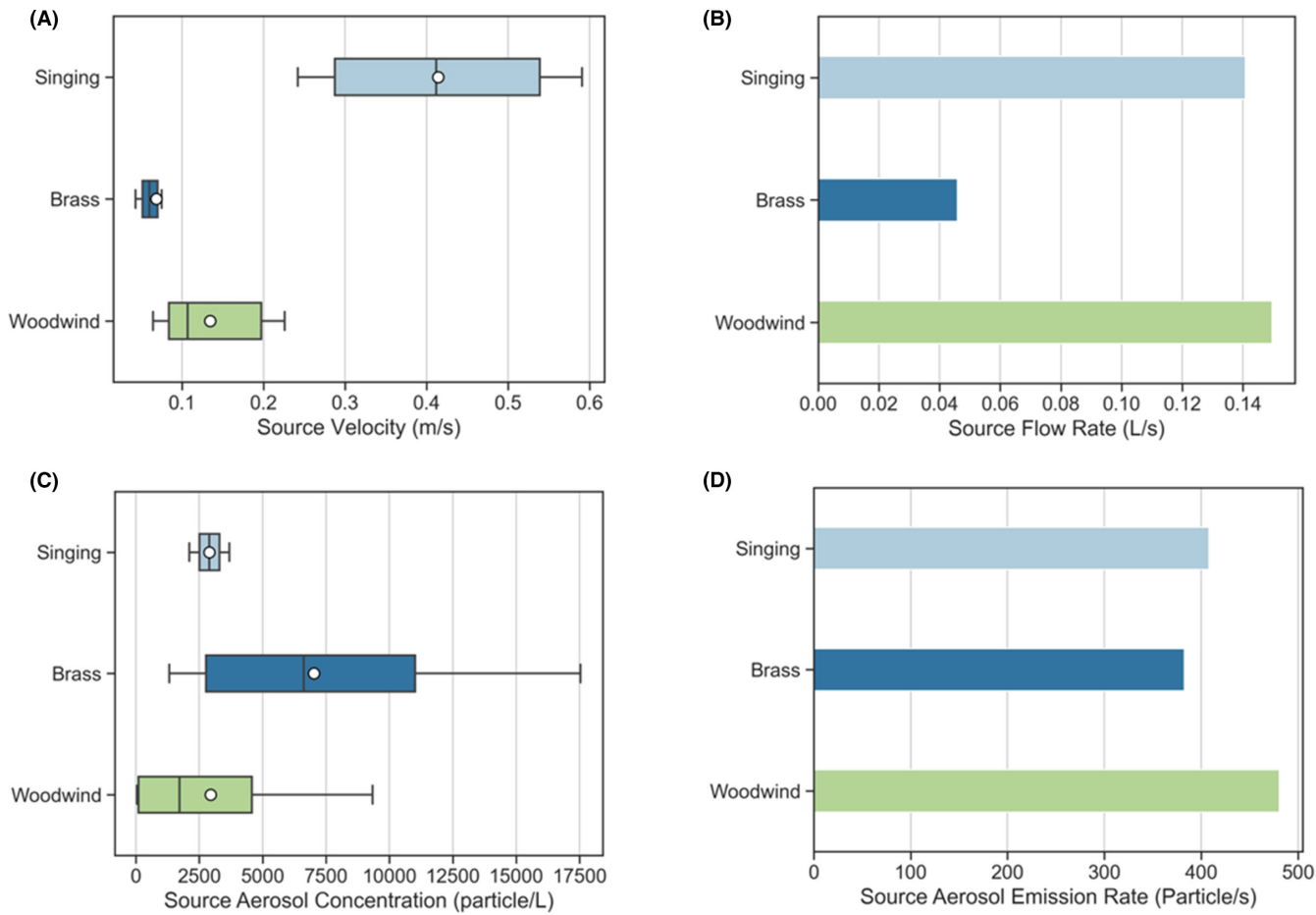


FIGURE 8 Source strength characterization of aerosol plumes from performance categories (singing, brass instrument and woodwind instrument). (A) Source velocity. (B) Source airflow rate. (C) Source aerosol concentration. (D) Source aerosol emission rate. (note: “source” refers to the time-averaged data collected at singer mouths or instrument outlets)

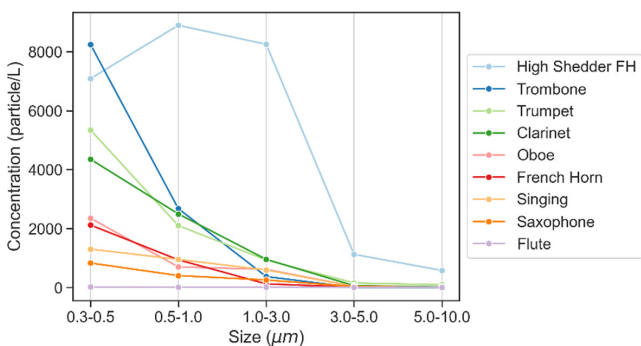


FIGURE 9 Size distribution of aerosol from musical performances

we normalized the source strength and convective transport capability data by their maximums to get values from zero to one. Secondly, the two normalized values were summed with weights to get the comprehensive characterization factor. The comprehensive characterization factor was classified into three categories: high (0.66–1), medium (0.33–0.66), and low (0–0.33). These bins are evenly distributed because they have equal importance. From

Table 6, the clarinet was classified as high. The flute, trombone, trumpet, “high shedder FH,” and singing were classified as medium. The oboe, saxophone, and French horn were classified as low. Figure 12 illustrates the comprehensive characterizations of the aerosol plumes. Figure 13 provides a qualitative visual comparison which allows simultaneous observation of plume size and averaged particle concentrations with the assumption of nearly real-time dispersion of aerosol.

3.4 | Mitigation methods

Mitigation methods, such as masks for singers and bell covers with MERV-13 filters for instruments, were tested in the experiments. Measurements were conducted in front of masks and bell covers, leakage areas were not considered in this study. Figure 14 shows the source aerosol concentration and the horizontal jet length comparison with and without mitigation methods for singing and clarinet performance. Based on the measurements, mitigation methods reduced source aerosol concentrations and the momentum of the airflow at the same time. All the other performances follow the

TABLE 4 Source characterization data of aerosol plumes from musical performances

Performance	Source Velocity (m/s)	Source Airflow Rate (L/s)	Source Aerosol Concentration (particle/L)	Source Aerosol Emission Rate (particle/s)
Flute	2.24	0.22	91	20
Oboe	0.06	0.02	3698	74
French horn	0.06	0.04	3197	128
Saxophone	0.11	0.10	1519	152
Singing	0.41	0.14	2899	406
Trumpet	0.09	0.05	8636	432
Trombone	0.05	0.05	11277	564
High Shedder FH	0.06	0.04	25960	1038
Clarinet	0.23	0.21	7894	1658

TABLE 5 Convective capability characterization data of aerosol plumes from musical performances

Performance	Horizontal instrument dimension (mm)	Horizontal jet length (mm)	Plume influence distance (mm)
French horn	0	253	253
Saxophone	0	319	319
Singing	0	604	604
Oboe	438	273	711
Trombone	400	338	739
Trumpet	483	331	814
Clarinet	467	407	874
Flute	660	522	1182

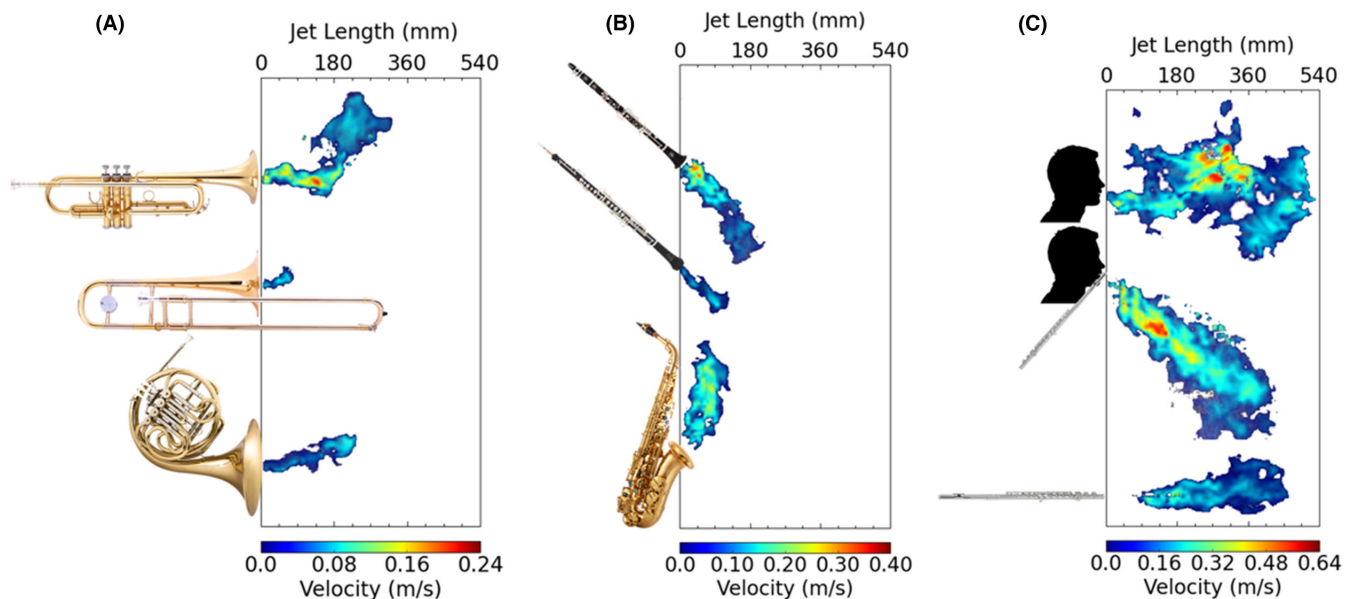


FIGURE 10 (A) Jets of the aerosol plumes from brass instruments. (B) Jets of the aerosol plumes from woodwind instruments. (C) Jets of the aerosol plumes from singing and flute. Note that the velocity scale is different in each panel

similar trend shown in the figure. According to Tables 7 and 8, for singing, wearing masks can bring source aerosol concentrations to the background level in front of a singer and reduce plume influence distances by 65%. For instruments, bell covers with filters can bring

source aerosol concentrations to the background level in front of the instrument bells and reduce plume influence distances by up to 57%. It is noteworthy that only a bell cover without filters cannot promise the reduction of the source aerosol concentration.

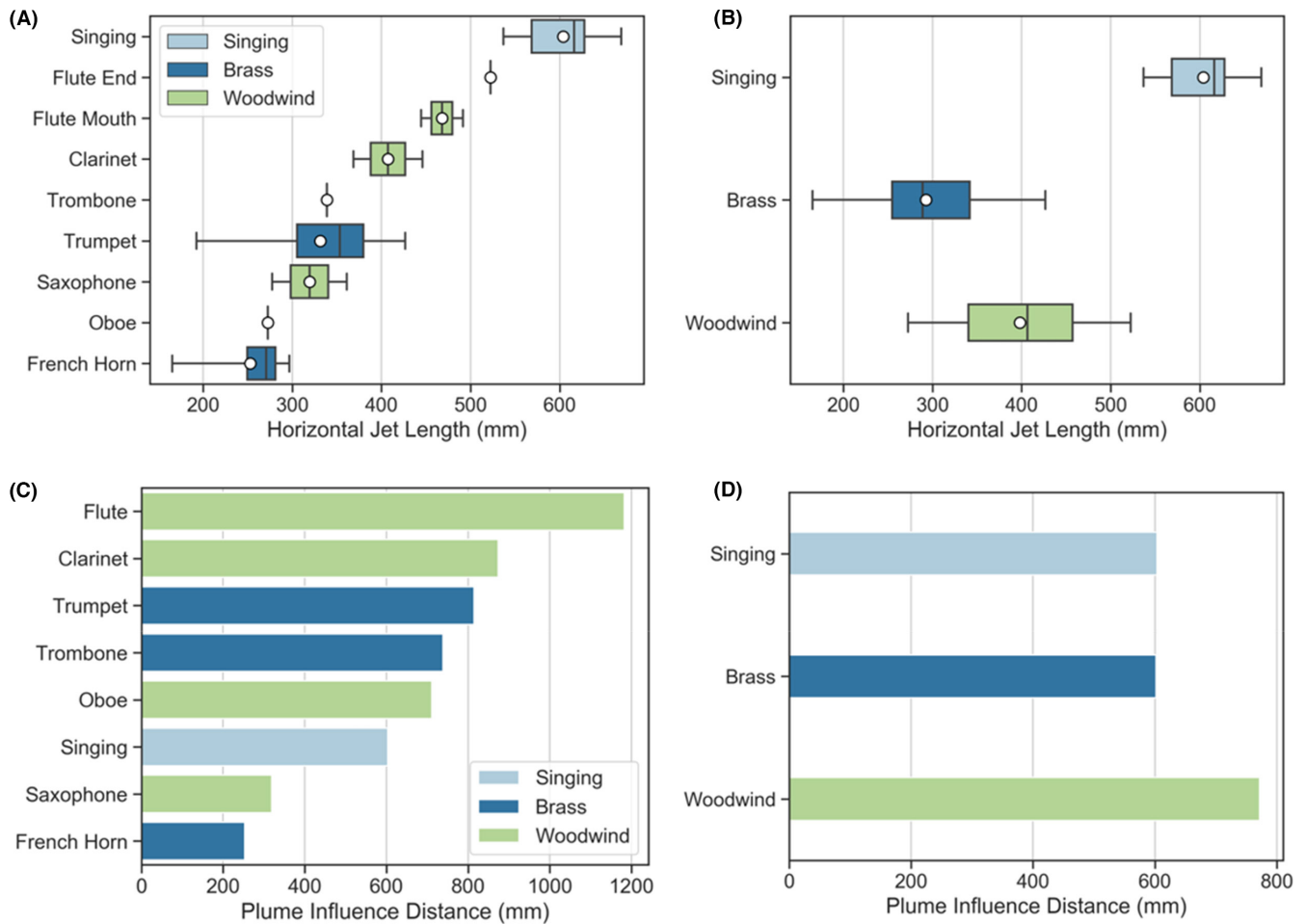


FIGURE 11 Convective transport capability characterization of aerosol plumes. (A) Horizontal jet lengths (musical performances). (B) Horizontal jet lengths (performance categories). (C) Plume influence distances (musical performance). (D) Plume influence distances (performance categories)

TABLE 6 Comprehensive characterization of aerosol plumes from musical performances

Performance	Aerosol emission rate (particle/s)	Normalized aerosol emission Rate	Plume influence distance (mm)	Normalized plume influence Distance	Comprehensive characterization Factor	Comprehensive characterization category
French horn	128	0.08	253	0.21	0.15	Low
Saxophone	152	0.09	319	0.27	0.18	
Oboe	74	0.04	711	0.60	0.32	
Singing	406	0.24	604	0.51	0.38	Medium
High Shedder FH	1038	0.63	253	0.21	0.42	
Trumpet	432	0.26	814	0.69	0.48	
Trombone	564	0.34	739	0.62	0.48	
Flute	20	0.01	1182	1	0.51	
Clarinet	1658	1	874	0.74	0.87	High

4 | DISCUSSIONS

The acoustics of musical performances may partly account for the generation of aerosol plumes. Brass instrument players produce sound by vibrating the lips,²⁹ while the woodwind instrument players produce sound by reed or air vibration,³⁰ and the singer vibrates vocal cords.³¹ The lip vibration may generate more aerosols than

the vibration of the reed and the vocal cord. This may be due to frequent accumulations of saliva in the instrument requiring release through water valves; brass instruments would then produce higher source aerosol concentrations than singing and wood instruments. Another cause could be condensations inside the brass tube due to the low surface temperature of brass instruments. In addition, a curved, long, and keyhole-less instrument means that more aerosols

would impact the walls than in the case of woodwinds. Moreover, the instrument's body resonates with the air flowing through it during performances²⁹; as a result, the vibration may lead to more aerosols being generated from the condensate on the walls. The tube of a woodwind instrument is usually short, straight, and has a number of keyholes on the tube where exhaled air may contact ambient air. Therefore, compared with the brass instrument, when playing a wood instrument, there is much less water condensations in the tube and aerosols can spread faster by air mixing.

The airflow of aerosol plumes from musical performances may also be influenced by the acoustics. The flute had the highest source air velocity and source airflow rate among the instruments because it produces sound by air vibration.³² The air jet formed by singing also had a relatively high source velocity, because it was directly released to indoor air without periodic valving actions of reeds or lips. The air jets formed by playing woodwind instruments with a single-reed had higher velocities than those of brass instruments. This may result from different interactions of the reed

and lips. A single-reed may have an opening area greater than one formed by lipping on a brass instrument, allowing more air flow. The oboe, which uses a double-reed, had the lowest velocity among woodwind instruments and the lowest source airflow rate among all the instruments. Compared with air jet instruments (flute) and single-reed instruments (clarinet and saxophone), double-reed instruments can generate much higher intraoral pressure with decreased source airflow rate for exhaled air because of the smaller gap between the blades of the reed.³³ Playing posture could be a source determinant for the horizontal length of the aerosol plume, as it would affect the direction of the jet. Furthermore, the length and shape of an air jet are determined by the physical characteristics of the instruments and the musicians' blowing techniques. Future research is needed to focus on the aerosol generation and airflow formation mechanisms influenced by the acoustics of musical performances.

Aerosol plumes created by the same instrument can vary widely in the source aerosol concentration, source velocity, and horizontal jet length for different human subjects. For the French horn, we measured source aerosol concentrations to be approximately 26000, 6700, and 1800 particle/L, respectively, for three human subjects. The high shedder had the highest concentration at about five times higher than the average concentration of the other two French horn players. Notably, this player was observed to more frequently remove condensations in the instrument in comparison with the other players. This could confirm that the accumulated condensation generates a significantly greater amount of aerosol or indicate that the player employed wetter lips, generating more aerosol at the mouthpiece. Therefore, even though singing and brass instruments produce a measurably lower risk on average than the woodwind instruments, it is possible to have an individual musician with high particle shedding rate and associated risk. However, the occurrence of this phenomenon was roughly 5% in this study, the sample was too small to make any conclusions regarding the general population of musicians. Different characteristics of aerosol plumes

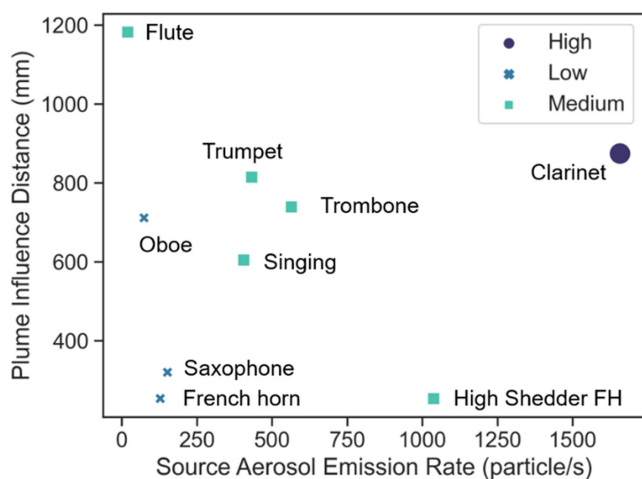


FIGURE 12 Comprehensive characterization of aerosol plumes

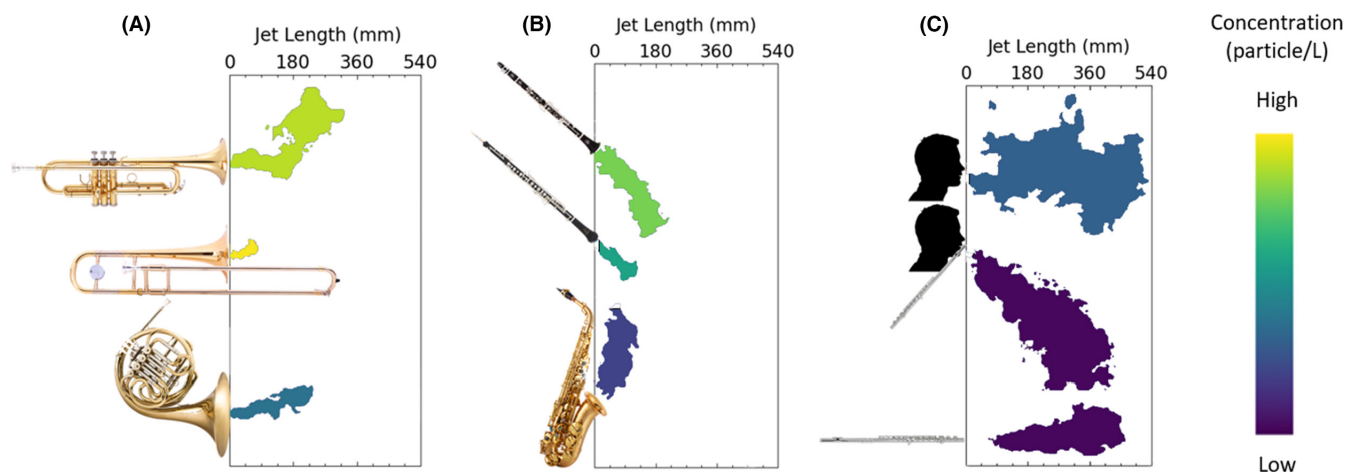


FIGURE 13 Qualitative comparison of measured average aerosol concentration in different jets of aerosol plumes. (The values of the concentrations can be found in Table 4)

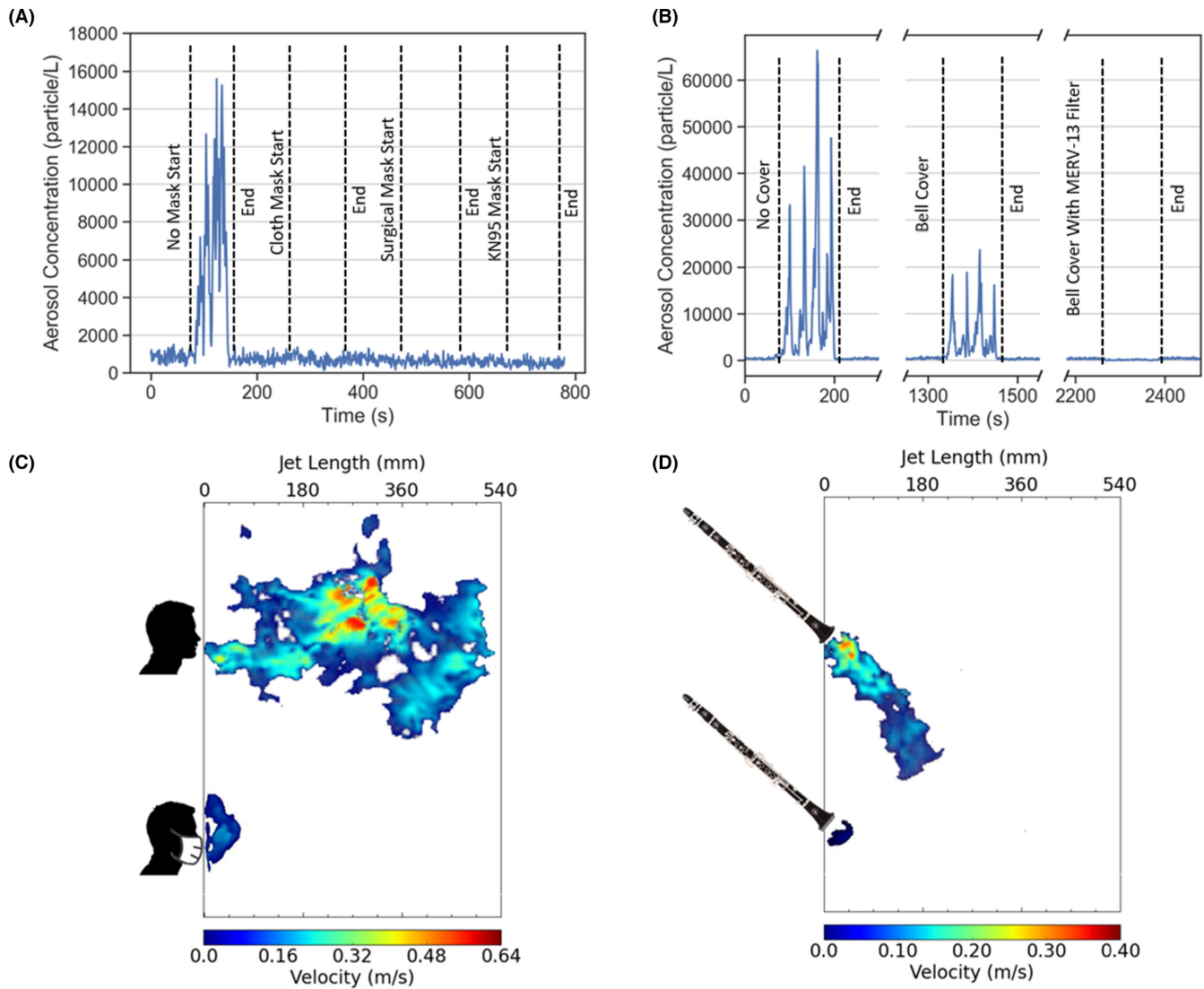


FIGURE 14 Source Aerosol concentration and horizontal jet length reduction by mitigation methods (singing and clarinet). (A) Real-time source aerosol concentration of aerosol plumes from singing (with/without mitigation methods). (B) Real-time source aerosol concentration of aerosol plumes from clarinet (with/without mitigation methods). (C) horizontal jet length comparison of singing (with/without mitigation methods). (D) horizontal jet length comparison of clarinet (with/without mitigation methods)

Category	Performance	No mitigation methods	With mitigation methods	Reduction percentage
Singing	Singing	2899	~0	100%
Brass instrument	French horn	3197	~0	100%
	High Shedder FH	25960	1657	94%
	Trumpet	8636	~0	100%
	Trombone	11277	~0	100%
Woodwind instrument	Clarinet	7894	~0	100%
	Saxophone	1519	~0	100%
	Oboe	3698	~0	100%

TABLE 7 Source Aerosol concentration (particle/L) reduction by mitigation methods

between each human subject might have been caused by diverse playing techniques and personal features. Further work is required to explore the variances caused by individual musician differences.

Implementing mitigation strategies is strongly recommended in musical performances to prevent airborne disease transmission. The comprehensive characterization factors and categorization can offer

TABLE 8 Horizontal jet length (mm) reduction by mitigation methods

Category	Performance	No mitigation methods	With mitigation methods	Reduction percentage
Singing	Singing	604	211	65%
Brass instrument	French horn	253	157	38%
	Trumpet	331	175	47%
Woodwind instrument	Clarinet	407	260	36%
	Saxophone	319	253	21%
	Oboe	273	117	57%

a reference for the protection strategies in musical performances. For example, if the musical performance has multiple instruments, which were listed in different categories, the decision maker can customize the protection strategy with the help of the comprehensive characterization. Higher level protection, such as a greater social distancing amount, could be implemented for the instruments with higher comprehensive characterization factors.

Aerosol measurements should consider the evaporation of particles because it influences particle diameters.^{34–37} The present study focused on particles with diameters between 0.3 μm and 10 μm because of their potential for aerosol transmission of viruses that is much more difficult to control than a spray of virus droplets characterized by larger particles. The measured air velocities were lower than 5 m/s, indoor air temperatures were at $22 \pm 2^\circ\text{C}$, and relative humidity levels were between 30% and 40%. Under these environmental conditions, the evaporation of particles is almost instantaneous,³⁴ so, particles were fully-evaporated before reaching the particle counter. Nicas et al.³⁸ identified that evaporation of aerosols rapidly reaches steady state with the particle diameter equal to half of its original size in typical indoor environmental conditions, similar to the experimental conditions in the present study. Therefore, the diameters of the sampled fully-evaporated aerosols were roughly half of their original diameters at the musician mouth openings or instrument outlets. However, high uncertainties are possible because the one-half shrinkage factor was a rough estimation from Nicas et al.,³⁸ and no other studies directly investigating the shrinkage of expelled respiratory particles were found.³⁸

Importantly, the transport of aerosols close to the source with resultant near-field aerosol concentrations is dominated by the source aerosol emission rate and a plume primarily driven by the initial air jet momentum. Further from the source, the transport of aerosols with resultant far-field aerosol concentrations is also impacted by the indoor airflow field. The present study focuses on characterizing the near-field aerosol plume properties because this is the first step in analyzing the far-field aerosol concentrations and transport. Future research could use the findings in the present study to predict and analyze far-field aerosol concentrations and transport.

Previous studies provided valuable data to evaluate our measurements. Importantly, in the present study, the data collection instrument allowed for collection of aerosols with particle diameters between 0.3 μm and 10 μm , which is a typical range for airborne

aerosols. Therefore, the comparative analysis between the current and existing studies used 0.3–10 μm range of aerosol diameters. Smaller aerosols than this range are also important,³⁹ but were not collected because the particle counter used in this study cannot collect particles smaller than 0.3 μm . Larger particles are droplets that were outside of the scope of the present study. During each of aerosol measurement experiments, the background concentration of particles was maintained at a very low level of 0.5 particle/ cm^3 . The saturation limit of the data collection device,⁴⁰ which is 210 particle/ cm^3 , was never reached during our experiments. In the comparison, most of our results are in the same magnitude as the results of Alsved et al.,⁷ Gregson et al.,¹⁵ He et al.,¹⁷ Stockman et al.,¹⁸ and McCarthy et al.¹⁹ The differences might be caused by different sampling sizes, sample variances, and different measuring equipment and setups in each experiment. For the source air velocity, our measurements are comparable with Stockman et al.,¹⁸ Bahl et al.,²⁰ and Becher et al.²¹ For the jet length, our measurements are in the same magnitude of the result from Becher et al.²¹ However, the plume influence distance is shorter than the result from Gantner et al.²³ The differences may be caused by different experiment methods and setups. Our experimental investigation could be limited by the number of human subjects. Moreover, for the convective transport characterization, the PIV imaging area may not fully cover the whole flow area of the musical performances with high velocities. Finally, some laser reflections by the instrument body during the PIV experiment, for example, trombone, could also influence the accuracy of the measurements.

5 | CONCLUSIONS

This study concluded that the characterization of aerosol plumes requires the source strength, characterized by the aerosol emission rate (brass 383 particle/s, singing 408 particle/s, woodwind 480 particle/s), and the convective transport capability, characterized by the plume influence distance (brass 0.6 m, singing 0.6 m, and woodwind 0.8 m), to indicate the risk of airborne virus transmission. The source strength, characterized by the source aerosol emission rate, requires the measurements of both source aerosol concentrations and source airflow rates. If only the source aerosol concentration is measured, important information about the air flow is ignored, so, the source strength characterization will be incomplete. For example, the clarinet showed medium source

aerosol concentration, but the highest source aerosol emission rate due to a high source airflow rate. Therefore, the source strength of aerosol plumes from clarinet would have been underestimated, if the source airflow rate had not been measured. From the results of the convective transport capability, the study found that the length and direction of the aerosol plumes in front of the musicians varied due to different instrument orientations and source velocities. To offer comprehensive information on the aerosol plume within a specified musical performance, it is necessary to comprehensively consider its source strength and convective transport capability simultaneously. As an example, playing flute generated aerosol plumes with the lowest source strength, but the highest convective transport capability. If we only considered the characteristic of the source strength, the risk assessment of the infection transmission caused by the aerosol plume from flute playing would be biased in an unsafe way. It is important to note that the comprehensive results show that airflow from musical performances is a critical component which influences the risk of airborne disease transmission. Overall, woodwind instruments showed the highest risk with around 20% higher source aerosol emission rates and 30% higher plume influence distances compared with the average of the same risk indicators for singing and brass instruments.

AUTHOR CONTRIBUTIONS

Lingzhe Wang involved in investigation, formal analysis, visualization, and writing—original draft. Tong Lin involved in investigation, validation, and writing—original draft. Hevander Da Costa involved in formal analysis, visualization, and writing—review and editing. Shengwei Zhu involved in conceptualization, methodology, writing—review and editing, and supervision. Tehya Stockman involved in investigation and writing—review and editing. Abhishek Kumar involved in investigation. James Weaver involved in conceptualization and funding acquisition. Mark Spede involved in conceptualization and funding acquisition. Donald K. Milton involved in supervision, COVID-19 testing, and writing—review and editing. Jean Hertzberg, Shelly L. Miller, and Marina E. Vance involved in supervision, writing—review and editing. Darin W. Toohey involved in supervision. Jelena Srebric performed conceptualization, methodology, writing—review and editing, supervision, resources, project administration, and funding acquisition.

ACKNOWLEDGEMENTS

The authors gratefully acknowledge the International Coalition led by the Performing Arts organizations, listed under the Funding Information, that commissioned this COVID-19 study. We are also thankful for the collaboration by the School of Music, University of Maryland, that allowed us to recruit musicians for the human subject part of this study (IRB 1622465-4).

CONFLICT OF INTEREST

The authors of this paper certify that they have NO affiliations with or involvement in any organization or entity with any

financial interest (such as honoraria; educational grants; participation in speakers' bureaus; membership, employment, consultancies, stock ownership, or other equity interest; and expert testimony or patent-licensing arrangements), or non-financial interest (such as personal or professional relationships, affiliations, knowledge, or beliefs) in the subject matter or materials discussed in this manuscript.

DATA AVAILABILITY STATEMENT

The data that support the findings of this study are available from the corresponding author upon reasonable request.

PEER REVIEW

The peer review history for this article is available at <https://publons.com/publon/10.1111/ina.13064>.

ORCID

Lingzhe Wang  <https://orcid.org/0000-0001-5657-4538>

Tong Lin  <https://orcid.org/0000-0002-5113-3423>

Shengwei Zhu  <https://orcid.org/0000-0002-0202-5514>

Tehya Stockman  <https://orcid.org/0000-0001-6613-9636>

Mark Spede  <https://orcid.org/0000-0002-8491-5042>

Donald K. Milton  <https://orcid.org/0000-0002-0550-7834>

Jean Hertzberg  <https://orcid.org/0000-0002-8984-6808>

Darin W. Toohey  <https://orcid.org/0000-0003-2853-1068>

Marina E. Vance  <https://orcid.org/0000-0003-0940-0353>

Shelly L. Miller  <https://orcid.org/0000-0002-1967-7551>

Jelena Srebric  <https://orcid.org/0000-0001-6825-5091>

REFERENCES

- Hamner L, Dubbel P, Capron I, et al. High SARS-CoV-2 attack rate following exposure at a choir practice—Skagit County, Washington, March 2020. *MMWR Morb Mortal Wkly Rep*. 2020;69:606-610.
- Lebrecht N. Concertgebouw chorus is devastated after pre-Covid Bach Passion. Slipped Disc. 2020.
- Colborne F. German choirs silenced as singing branded virus risk. Yahoo. 2020.
- Charlotte N. High rate of SARS-CoV-2 transmission due to choir practice in France at the beginning of the COVID-19 pandemic. *J Voice*. 2020;(In press). doi:10.1016/j.jvoice.2020.11.029
- Furuse Y, Sando E, Tsuchiya N, et al. Clusters of coronavirus disease in communities, Japan, January-April 2020. *Emerging Infect Dis*. 2020;26(9):2176-2179.
- Fautré W. COVID-19: treatment of clusters in Protestant Churches and the Shincheonji Church in South Korea. A comparative study. *J CESNUR*. 2020;4:86-100.
- Alsved M, Matamis A, Bohlin R, et al. Exhaled respiratory particles during singing and talking. *Aerosol Sci Technol*. 2020;54:1245-1248.
- Mürbe D, Kriegel M, Lange J, Schumann L, Hartmann A, Fleischer M. Aerosol emission of adolescents voices during speaking, singing and shouting. *PLoS One*. 2021;16:e0246819.
- Bourouiba L. Turbulent gas clouds and respiratory pathogen emissions: potential implications for reducing transmission of COVID-19. *JAMA - J Am Med Assoc*. 2020;323:1837-1838.
- Sun C, Zhai Z. The efficacy of social distance and ventilation effectiveness in preventing COVID-19 transmission. *Sustainable Cities Soc*. 2020;62:102390.

11. Hedworth HA, Karam M, McConnell J, Sutherland JC, Saad T. Mitigation strategies for airborne disease transmission in orchestras using computational fluid dynamics. *Sci Adv*. 2021;7:eabg4511.
12. Rosti ME, Olivieri S, Cavaola M, Seminara A, Mazzino A. Fluid dynamics of COVID-19 airborne infection suggests urgent data for a scientific design of social distancing. *Sci Rep*. 2020;10:22426.
13. Stadnytskyi V, Bax CE, Bax A, Anfinrud P. The airborne lifetime of small speech droplets and their potential importance in SARS-CoV-2 transmission. *Proc Natl Acad Sci USA*. 2020;117:11875-11877.
14. Abkarian M, Mendez S, Xue N, Yang F, Stone HA. Speech can produce jet-like transport relevant to asymptomatic spreading of virus. *Proc Natl Acad Sci USA*. 2020;117:25237-25245.
15. Gregson FKA, Watson NA, Orton CM, et al. Comparing aerosol concentrations and particle size distributions generated by singing, speaking and breathing. *Aerosol Sci Technol*. 2021;55:681-691. doi:10.1080/02786826.2021.1883544
16. Lai K-M, Bottomley C, McNerney R. Propagation of respiratory aerosols by the vuvuzela. *PLoS One*. 2011;6:e20086.
17. He R, Gao L, Trifonov M, Hong J. Aerosol generation from different wind instruments. *J Aerosol Sci*. 2021;151:105669.
18. Stockman T, Zhu S, Kumar A, et al. Measurements and simulations of aerosol released while singing and playing wind instruments. *ACS Environ Au*. 2021;1(1):71-84.
19. McCarthy LP, Orton CM, Watson NA, et al. Aerosol and droplet generation from performing with woodwind and brass instruments. *Aerosol Sci Technol*. 2021;55:1277-1287.
20. Bahl P, de Silva C, Bhattacharjee S, et al. Droplets and aerosols generated by singing and the risk of coronavirus disease 2019 for choirs. *Clin Infect Dis*. 2021;72:e639-e641.
21. Becher L, Gena AW, Alsaad H, Richter B, Spahn C, Voelker C. The spread of breathing air from wind instruments and singers using schlieren techniques. *Indoor Air*. 2021;31:1798-1814. doi:10.1111/ina.12869
22. Abraham A, He R, Shao S, et al. Risk assessment and mitigation of airborne disease transmission in orchestral wind instrument performance. *J Aerosol Sci*. 2021;157:105797. doi:10.1016/j.jaero sci.2021.105797
23. Gantner S, Echternach M, Veltrup R, et al. Impulse dispersion of aerosols during playing wind instruments. *PLoS ONE*. 2022;17(3). doi:10.1101/2021.01.25.20248984
24. Papineni RS, Rosenthal FS. The size distribution of droplets in the exhaled breath of healthy human subjects. *J Aerosol Med*. 1997;10(2):105-116. www.liebertpub.com
25. Asadi S, Wexler AS, Cappa CD, Barreda S, Bouvier NM, Ristenpart WD. Aerosol emission and superemission during human speech increase with voice loudness. *Sci Rep*. 2019;9:2348.
26. Asadi S, Wexler AS, Cappa CD, Barreda S, Bouvier NM, Ristenpart WD. Effect of voicing and articulation manner on aerosol particle emission during human speech. *PLoS One*. 2020;15:e0227699.
27. Becher L, Voelker C, Rodehorst V, Kuhne M. Background-oriented Schlieren technique for two-dimensional visualization of convective indoor air flows. *Opt Lasers Eng*. 2020;134:106282.
28. Raffel M, Willert CE, Wereley ST, Kompenhans J. *Particle image velocimetry: A practical guide*. 2nd ed. Springer; 2007.
29. Fox F. *Essentials of brass playing: An explicit, logical approach to important basic factors that contribute to superior brass instrument performance*. Alfred Publishing Company; 1978.
30. Eargle JM. Acoustics of woodwind instruments. In: *Music, sound, and technology* 105-124. Springer US; 1995. doi:10.1007/978-1-4757-5936-5_6
31. Doscher BM. *The functional unity of the singing voice*; 1994.
32. Coltman JW. Sounding mechanism of the flute and organ pipe. *J Acoust Soc Am*. 1968;44:983-992.
33. Wolfe J. *Double reed acoustics: Oboe, bassoon and others*. The University of New South Wales; n.d. <https://newt.phys.unsw.edu.au/jw/double-reed-acoustics.html>
34. Xie X, Li Y, Chwang ATY, Ho PL, Seto WH. How far droplets can move in indoor environments—revisiting the Wells evaporation-falling curve. *Indoor Air*. 2007;17:211-225.
35. Liu L, Wei J, Li Y, Ooi A. Evaporation and dispersion of respiratory droplets from coughing. *Indoor Air*. 2017;27:179-190.
36. Johnson GR, Morawska L, Ristovski ZD, et al. Modality of human expired aerosol size distributions. *J Aerosol Sci*. 2011;42:839-851.
37. Morawska L, Johnson GR, Ristovski ZD, et al. Size distribution and sites of origin of droplets expelled from the human respiratory tract during expiratory activities. *J Aerosol Sci*. 2009;40:256-269.
38. Nicas M, Nazaroff WW, Hubbard A. Toward understanding the risk of secondary airborne infection: emission of respirable pathogens. *J Occup Environ Hygiene*. 2005;2:143.
39. Holmgren H, Ljungström E, Almstrand AC, Bake B, Olin AC. Size distribution of exhaled particles in the range from 0.01 to 2.0 μm . *J Aerosol Sci*. 2010;41:439-446.
40. TSI Incorporated. AEROTRAK™ Handheld Airborne Particle Counter Operation Manual; 2010.

SUPPORTING INFORMATION

Additional supporting information may be found in the online version of the article at the publisher's website.

How to cite this article: Wang L, Lin T, Da Costa H, et al. Characterization of aerosol plumes from singing and playing wind instruments associated with the risk of airborne virus transmission. *Indoor Air*. 2022;32:e13064. doi:10.1111/ina.13064